Journal of Environmental Management 351 (2024) 119834

Contents lists available at ScienceDirect

Journal of Environmental Management

journal homepage: www.elsevier.com/locate/jenvman

Research article

Optimization of two-phase synthesis of Fe-hydrochar for arsenic removal from drinking water: Effect of temperature and Fe concentration

Fabrizio Di Caprio [a,*], Pietro Altimari [a], Maria Luisa Astolfi [a,b], Francesca Pagnanelli [a,**]

[a] Dipartimento di Chimica, Università Sapienza di Roma, Piazzale Aldo Moro 5, 00185, Rome, Italy
[b] CIABC, Università Sapienza di Roma, Piazzale Aldo Moro 5, 00185, Rome, Italy

ARTICLE INFO

Keywords:
Hydrochar
Olive pomace
Arsenic removal
Fe coating
Composite adsorbent
Biochar

ABSTRACT

Arsenic-contaminated water is a global concern that demands the development of cost-effective treatments to ensure a safe drinking water supply for people worldwide. In this paper, we report the optimization of a two-phase synthesis for producing a hydrochar core from olive pomace to serve as support for the deposition of Fe-hydroxide, which is the active component in As(V) removal. The operating conditions considered were the initial concentration of Fe in solution in the hydrothermal treatment (phase I) and the temperature of Fe precipitation (phase II). The obtained samples were characterized for their elemental composition, solid yield, mineral content (Fe and K), phenol release, As(V) sorption capacity, and sorbent stability.

Correlation analysis revealed that higher Fe concentrations (26.8 g/L) ensured better carbonization during hydrothermal treatment, increased arsenic removal, reduced concentrations of phenols in the final liquid, and improved stability of the sorbent composite. On the other hand, the temperature during Fe precipitation (phase II) can be maintained at lower levels (25–80 °C) since higher temperatures yielded lower adsorption capacity. Regression analysis demonstrated the significance of the main effects of the parameters on sorption capacity and provided a model for selecting operating conditions (Fe concentration and phase II temperature) to obtain composite sorbents with tailored sorption properties.

1. Introduction

Arsenic contamination of groundwater is a relevant health problem due to the carcinogenic activity of this element, even in trace quantities. Accordingly, the World Health Organization recommended a limit of 10 μg/L for As in drinking water (Ahsan, 2011), and the same strict limit is established by the US Environmental Protection Agency (EPA 815) and the EU directive (98/83/CE).

Arsenic concentration often exceeds this limit in groundwater due to the natural leaching from As-containing ores, and anthropogenic contaminations related to the discharge and disposal of As-containing wastes (Katsoyiannis et al., 2015; Medunić et al., 2020; Ungureanu et al., 2015). In these cases, contaminated groundwater requires to be treated before its distribution as drinking water, to reduce As below the allowance limit.

Arsenic can be present in groundwater as As(V) and As(III) according to the oxidation/reduction potential (ORP) and pH conditions (Sappa et al., 2014; Sorg et al., 2014; Wang and Mulligan, 2006). Arsenic concentrations above the EU limit (50 - 1500 μg/L) have been reported in several regions of Italy, Belgium, Greece, Croatia, Hungary, Germany and other countries (Katsoyiannis et al., 2015).

The contamination generally impacts delimited areas. Small municipalities have issues on installing and operating the required water treatment plants. Indeed, in 2010 there were still 128 municipalities in Italy with As concentration in tap water higher than the EU limit, which prevented water supply for about 1,000,000 citizens (Bruxelles, 2010). A monitoring in the Lazio region (Italy) found up to 345 defaults per year in 69 municipalities in the Viterbo area (years 2016–2018). These defaults correspond to 20–30% of the samples monitored ("Ambiente - ARPA Lazio," 2018; European Commission, 2019). Similar problems were experienced in other countries (Jovanovic et al., 2011).

Different technologies are available for As removal, such as chemical precipitation/coagulation, adsorption, ion exchange, and membrane technologies (Jadhav et al., 2015). Adsorption is deemed the most effective method because it is characterised by higher efficiency and operative and investment costs lower than other methods, such as

* Corresponding author.
** Corresponding author.
E-mail addresses: fabrizio.dicaprio@uniroma1.it (F. Di Caprio), francesca.pagnanelli@unirom1.it (F. Pagnanelli).

https://doi.org/10.1016/j.jenvman.2023.119834
Received 2 August 2023; Received in revised form 15 November 2023; Accepted 21 November 2023
Available online 20 December 2023

membrane technologies (Cope et al., 2014).

Several adsorbent materials, such as clays and (hydro)oxides (e.g. Fe_2O_3, Fe_3O), have been tested due to the tendency of As to form complexes on the surface of metal oxy-hydro groups of Fe, Al, and Mn (Jadhav et al., 2015; Zubair et al., 2020). Iron oxide nanoparticles present high adsorption capacity among the different sorbent materials (Luong et al., 2018). Due to problems related with the use of nanomaterials (pressure drop), iron oxides are used as granulated materials in fixed column reactors (GFH, Granulated Ferric Hydroxide). Granulation is needed to avoid problems such as pressure drop in columns and easy separation of solid sorbents from treated water (Driehaus, 2002). GFH is a widely used material among the existing treatment plants, but the present high cost prevents its widespread application in contaminated areas, especially in rural areas and developing countries where no treatment of As-contaminated water is performed, with more than 140 million people exposed to water with As $>$ 10 μg/L (WHO TEAM Water and Sanitation, 2018).

Different types of composite sorbents have been developed recently to remove As and reduce the operating costs of this treatment. These composites are made up of carbon-like cores impregnated or coated with iron oxides using agro-industrial wastes for producing the carbon core and thus reducing the amount of primary materials (Fe oxides) used with respect to GFH. Carbon-cores can be produced by different thermal treatments starting from conventional active carbons impregnated with iron oxides (Chang et al., 2010) and arriving at the innovative choice of using as carbon core biochar (Cope et al., 2014; He et al., 2018; Wang et al., 2015; Wei et al., 2019) and hydrochar (Capobianco et al., 2020; Chen et al., 2022; Di Caprio et al., 2022; Mourão et al., 2022; Zhang et al., 2022). These materials are obtained by milder thermal treatments such as dry pyrolysis (biochar) and hydrothermal carbonization (hydrochar). Hydrothermal carbonization (HTC) is an extremely promising treatment for wet wastes as it does not require preliminary drying (as pyrolysis), allowing the obtainment of both solid and liquid phases, which can be further exploitable. HTC is performed in closed vessels at temperatures from 150 to 350 °C, lower than pyrolysis (400–600 °C), under autogenous pressure (2–20 MPa) (Azzaz et al., 2020). In these conditions, carbon-like materials are obtained as a solid phase along with a sterilized solution containing organic substances, which can be further valorised for antioxidant production (Gimenez et al., 2020) biotechnological feed (Tarhan et al., 2021) or biofertilizer, being a sterile solution rich in nutrients (Wang et al., 2023). HTC exploits the unconventional solvent characteristics of subcritical water (decreased dielectric constant and increased acid constant) to promote a cascade of reactions including hydrolysis, dehydration, decarboxylation, aromatization, condensation, depolymerisation and Fischer-Tropsch synthesis (Libra et al., 2011). The final characteristics of hydrochar strongly depend upon the feed material used and the operating conditions adopted such as temperature, time, and solid/liquid ratio. Hydrochar generally presents 55–74% carbon (Missaoui et al., 2017) and a high concentration of oxygenated groups (such as carboxylic, lactonic, and phenolic groups) (Azzaz et al., 2022) amenable for sorption or further functionalization. Both biochar and hydrochar, if used for sorbent applications, generally require an additional step of activation to increase the surface area. Site functionalization, and adding other active components, have been reported as strategies to increase As sorption capacity, as with the addition of iron oxides (Chen et al., 2022).

Considering agro-industrial wastes, olive pomace is largely produced in the Mediterranean basin where there is a large part of the global production of olive oil (Agri E, 2023). Olive pomace has already been tested for possible applications as adsorbent material for metal removal after chemical and thermal treatment (Akar et al., 2009; Martín-Lara et al., 2008; Nuhoglu and Malkoc, 2009; Pagnanelli et al., 2003, 2008). More recently olive pomace was used as feed in hydrothermal carbonization for hydrochar production aiming mainly at solid biofuel production (Álvarez-Murillo et al., 2015; Başakçılardan Kabakcı and Baran, 2019; Benavente et al., 2015; Gimenez et al., 2020; Missaoui et al., 2017; Volpe and Fiori, 2017). Only one work investigated using olive pomace hydrochar directly as sorbent material for pollutant removal, reporting the sorption towards methylene blue (Alshareef et al., 2021). Regarding the use of hydrochar from olive pomace to produce Fe-composite sorbents for As removal, only the previous works of our research group are present in the literature (Capobianco et al., 2020; Di Caprio et al., 2022; Mourão et al., 2022). In particular, these previous works reported that hydrothermal carbonization of olive pomace and formation of Fe precipitates required different optimum pH conditions, thus imposing a two-phase synthesis. The first stage of this process (phase I) was optimized by studying the effect of pH by testing different H_2SO_4 concentrations, at different reaction times, finding a positive effect of acid pH on carbonization and an optimal reaction time of 30 min (Di Caprio et al., 2022). The second phase of the process (phase II), in which a base is added to precipitate Fe oxides, was scarcely studied. Some studies working with biochar (from conventional pyrolysis) optimized the operative conditions to functionalize the biochar with Fe compounds (Xu et al., 2021, 2022, 2023). However, in these latter studies the functionalization was achieved by the addition of Fe to the solution and water vaporization. In the present study, functionalization is, in contrast, achieved by inducing the iron precipitation without water vaporization. This way, after the Fe-hydrochar recovery, the residual HTC solution can be used as fertilizer, thus increasing the circularity of the process. To evaluate the feasibility of this strategy, it is important to evaluate how process parameters affect not only the Fe-hydrochar characteristics but also the quality of the residual HTC process water. Such an analysis, which cannot be inferred from previous studies achieving the Fe functionalization by water vaporization, constitutes an important contribution of the present study.

In particular, the main novelty of the present work is analysing the effect of Fe concentration and temperature of phase II on the performance of the process, the quality of the produced Fe-coated hydrochar, and of the residual process water. Indeed, Fe-precipitation efficiency could be affected by the organic compounds released in the liquid phase during phase I of the HTC process. In addition, regarding the previous two-phase synthesis, in this study, H_2SO_4 is not added during hydrothermal carbonization because Fe^{3+} ions are exploited as the sole acid.

2. Materials and methods

2.1. Materials

Olive pomace was collected from a two-phase olive oil mill plant at Roccasecca dei Volsci (LT, Italy). Olive pomace was centrifuged at 5000 rpm for 10 min, and the pellet was dried at 105 °C for about 4 d until constant weight. Dried pomace was manually ground in an agate mortar and finally sieved to remove particles $>$ 1 mm, mainly composed of olive stones and leaves. $FeCl_3 \bullet 6H_2O$ (99%), KOH (>99%) and KH_2AsO_4 (98–102%) were purchased from Merck/Sigma Aldrich.

2.2. Two-stage synthesis of Fe-coated hydrochar

Fe-coated hydrochar samples were prepared according to the two-phase process, as reported in Fig. 1A. Hydrochar was synthesized by mixing 5.0 g of olive pomace with 20 mL of aqueous solution (25% w/v) in a 100 mL polytetrafluoroethylene (PTFE) vessel. HTC was performed using different aqueous solutions at four levels of Fe^{3+} concentration (0, 6.7, 13.4, and 26.8 g/L).

The biomass suspensions were treated at 200 °C for 30 min using the Milestone Laboratory Microwave System Labstation. The reaction time was set to 30 min since a preliminary test indicatedit was enough to attain a stationary phase (Fig. S1). After cooling, the vessels were opened and left for 30 min under the fume hood. Different volumes of KOH 6.5 M were then added to the suspensions to attain the same pH in phase II of Fe precipitation: 2.1 mL for suspensions without Fe(III), 3.3

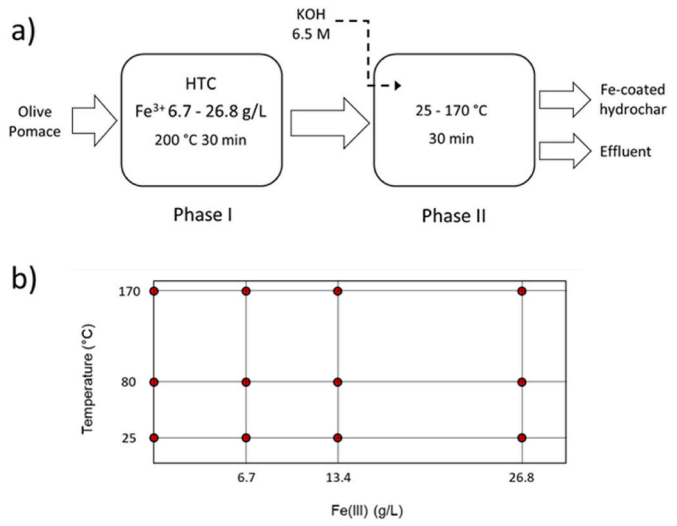

Fig. 1. a) Block diagram of the preparation process carried out to obtain the Fe-hydrochar; b) scheme of the treatments of the factorial design performed for Fe-hydrochar preparation. Each treatment was replicated three times.

mL for suspensions with 6.7 g/L of Fe(III), 4.6 mL for 13.4 g/L of Fe(III), and 7.0 mL for 26.8 g/L of Fe(III). Fe(III) was chosen as the source of Fe because of its higher acidity than Fe(II).

For each Fe(III) level, three different temperature levels were tested during phase II: 25, 80, and 170 °C. The reactor was maintained at 25 and 80 °C with a thermostatic bath (ARGO LAB C B 5–10) under magnetic stirring, while at 170 °C with the Milestone Laboratory Microwave System Labstation. All precipitation tests lasted 30 min.

For each treatment, the solid product obtained (Fe-coated hydrochar, m_{HC}) was recovered by vacuum filtration through 8–12 μm filter paper (VWR International, cat. No 516-0264) and finally dried at 105 °C. The obtained permeates were stored at - 20 °C for further analysis.

For each treatment, the whole HTC procedure was repeated three times in independent vessels (n = 3). Then the complete set of results consists of a complete factorial design with 4 levels of Fe(III) concentration and 3 levels of temperature, with a total of 3 × 4 = 12 treatments (Fig. 1B).

2.3. Characterization of solids and liquids

The elemental composition of solid samples was determined by CHNS analysis carried out by an elemental analyzer (EA 1110 CHNS/O). Fe and K concentrations in the solid samples were determined by acid digestion: 100 mg of hydrochar were mixed with 8 mL HNO_3 65% and 2 mL H_2O_2 30% in a 100 mL PTFE vessel, then heated by microwaves according to the following digestion program: 2 min from 25 °C to 85 °C, 5 min from 85 °C to 145 °C, 3 min from 145 °C to 200 °C, 20 min at 200 °C and 30 min for cooling. At the end, sample solutions were diluted and analysed for Fe and K content by Inductively Coupled Plasma Optical emission Spectrometry (ICP-OES; Vista MPX CCD Simultaneous, Varian, Victoria, Mulgrave, Australia) in axial view mode and equipped with a cyclonic glass chamber, as described in a previous work (Capobianco et al., 2020). Liquid samples were analysed for final pH with a glass electrode (InLab® Expert Pro ISM®, Mettler Toledo) calibrated with standard solutions at pH 4.0, 7.0, and 9.0, and for total phenols (as tyrosol equivalents) by the Folin-Ciocalteau method (Di Caprio et al., 2018). The stability in water of the solid hydrochar sample obtained was determined by suspending 20 mg of sample (m_0) in 20 mL of water maintained under stirring for 24 h at pH 8. Then the whole suspension was filtered through 0.7 μm filters and dried at 105 °C to determine the residual mass (m_f). Sample stability in water was finally calculated by Eq. (1).

$$\%\ \text{Stability} = \frac{m_f}{m_0} 100 \tag{1}$$

2.4. Arsenic adsorption tests

Arsenic adsorption tests were carried out for all solid samples produced. 20 mg of solid were added inside 50 mL glass bottles filled with 20 mL solution containing 15 mg/L As(V) prepared dissolving KH_2AsO_4 in distilled water. The suspension was magnetically stirred (700 rpm) at room temperature for 20 h to attain equilibrium conditions, as previously reported (Capobianco et al., 2020). The pH was set at 5.0 ± 0.2 during the test by adjusting it with 0.05 M NaOH or 0.05 M HCl. Finally, an aliquot of the supernatant obtained after centrifugation (5000 rpm × 5 min) was collected and stored at - 20 °C before the analytical determination of As, K, Fe, and C by ICP-OES as previously reported (Capobianco et al., 2020). The biomass remaining at the end of the adsorption test (m_R) was measured by filtering the whole suspension through 0.7 μm filters and subsequently dried at 105 °C.

2.5. Estimated output variables

Starting from the experimental tests and characterizations reported above, 15 different output variables were used in statistical analysis. In the following, these variables are described.

- Corrected %C (%C′): % amount of C in the solid product was corrected for the presence of Fe and K compounds, considering the mass content of Fe and K determined by acid digestion and assuming Fe $(OH)_{2.7}Cl_{0.3}$ and KCl as solid species according to thermodynamic simulations (Fig. S2) (Eq. (2)).

$$\%C' = \frac{\%C \times m_{HC}}{m_{HC} - m_{Fe(OH)_{2.7}Cl_{0.3}} - m_{KCl}} \tag{2}$$

where m_{HC}, $m_{Fe(OH)_{2.7}Cl_{0.3}}$ and m_{KCl} are the mass of hydrochar, Fe and K solid species.

- Corrected %N (%N′): % amount of N in the solid product corrected for the presence of Fe and K compounds, calculated as for C.
- Corrected %H (%H′): % amount of H in the solid product corrected for the presence of Fe and K compounds, calculated as for C.
- Corrected HTC yield (yield %'): estimated net weight of hydrochar material in the recovered solid without Fe and K compounds whose amount is estimated by Eq. (3).

$$yield\ \%' = \frac{m_{HC} - m_{Fe(OH)_{2.7}Cl_{0.3}} - m_{KCl}}{m_B} \times 100 \tag{3}$$

where m_B is the mass of the initial biomass added to the HTC vessel.

- %C yield: estimated considering elemental analysis in initial biomass and final products by Eq. (4).

$$\%C\ yield = \frac{\%C_{HC} \times m_{HC}}{\%C_B \times m_B} \times 100 \tag{4}$$

where $\%C_{HC}$ and $\%C_B$ are the content of C in the final Fe-coated hydrochar and initial biomass, respectively.

- %N yield: it was estimated as for C yield, considering elemental analysis in the initial biomass and in the final Fe-hydrochar.
- Fe/HTC (mg/g): Fe content in the final Fe-hydrochar.
- K/HTC (mg/g): K content in the final Fe-hydrochar.
- Phenols (mg/L): phenol concentration in the water solution recovered at the end of the process.
- HTC pH: pH measured in the water solution recovered at the end of the process.

- % Stability: % weight of solid collected after stirring it in water at controlled pH (Eq. (1)).
- q (mg/g): sorption of As(V) onto the solid hydrochar obtained at the end of the adsorption test (Eq. (5)).

$$q = \frac{V\left(C_i - C_f\right)}{m_R} \tag{5}$$

with C_f and C_i the final and initial As(V) concentration measured at the beginning and at the end of the adsorption test, and m_R is the biomass at the end of the adsorption test. In this way, the fraction of soluble mass released during the adsorption test was not included in the calculation of q.

- Fe release (mg/L): Fe concentration in solution at the end of the sorption experiment.
- K release (mg/L): K concentration in solution at the end of the sorption experiment.
- C release (mg/L): C concentration in solution at the end of the sorption experiment.

All values of the output variables cited before are available as supplementary file.

2.6. Statistical analysis of data

Correlation analysis was performed calculating for each couple of variables x,y reported in 2.5 section the correlation coefficient c_{xy} (Eq. (6)).

$$c_{xy} = \frac{\sum[(x_i - \bar{x})(y_i - \bar{y})]}{\sqrt{\sum (x_i - \bar{x})^2 \sum (y_i - \bar{y})^2}} \tag{6}$$

where x_i and y_i are the experimental results, and $\bar{x}$ and $\bar{y}$ are the means of the experimental results.

For each couple of variables, a hypothesis test was performed regarding the significance of correlation.

Regression analysis was performed considering a two factors model including an intercept (β_0), two coefficients for the two factors (β_1 for temperature T, and β_2 for [Fe]), and one coefficient for the interaction (β_3) according to Eq. (7).

$$y = \beta_0 + \beta_1 T + \beta_2 [Fe] + \beta_3 (T - \overline{T})([Fe] - \overline{[Fe]}) \tag{7}$$

The terms $\overline{T}$ and $\overline{[Fe]}$ indicate the average values determined from the extreme levels tested, namely 97.5 °C and 17.25 g/L for phase II temperature and Fe(III) concentration, respectively. The significance of each coefficient was determined by a *t*-test, considering $\beta_i = 0$ as a null hypothesis.

Statistical analysis of data was performed using JMP software.

3. Results and discussion

3.1. Preliminary reasoning about the elaborated output variables

The experimental design was a factorial design including the investigation of two factors: Fe(III) concentration in solution during hydrothermal treatment (levels of Fe(III) concentration: 0, 6.7, 13.4, and 26.8 g/L), and temperature of phase II during Fe precipitation for producing Fe-hydrochar (levels of phase II temperature: 25, 80 and 170 °C) (Fig. 1).

Under hydrothermal treatments, lignocellulosic materials, such as olive pomace, undergo reactions of hydrolysis, dehydration, decarboxylation, and polymerisation occurring at different degrees according to the operating conditions, thus leading to different final yields in solid products and different compositions of the residual solutions (Fernández-Sanromán et al., 2021). Hydrolysis determines an increased concentration of soluble compounds in the water phase and a reduction of the final solid yield, while dehydration and decarboxylation reactions determine a reduced final solid yield along with a decrease in the solid hydrogen and oxygen content. The repolymerisation of soluble compounds by condensation reactions determines an increased final solid yield. Still, these reactions can occur only if the hydrolysis of organic compounds (able to condense) has occurred before. Hydrolysis reactions play a key role in hydrochar composition and the degree of reaction can be regulated by adding acid reactants during HTC and/or by increasing the treatment temperature (Álvarez-Murillo et al., 2015). Protons provided by acids can even catalyse the de-hydration of alcoholic groups, such as those of sugars. In this work, the protons needed for hydrolysis and de-hydration of biomass are furnished by the hydrolysis reaction of Fe^{3+} ($K_a = 6 \bullet 10^{-3}$) with water, thus having already in the system iron ions for phase II.

The effect of increased Fe^{3+} concentration in solution is then related to increased hydrolysis and de-hydration (carbonization) power and increased amount of active solids in the sorption process. As for the first effect, the initial pH of the different Fe^{3+} solutions was 1.78, 1.65, and 1.0 for 6.7, 13.4, and 26.8 g/L Fe^{3+}, respectively. This concentration range allows, for higher Fe^{3+} concentrations, pH comparable to those previously attained using H_2SO_4 (Di Caprio et al., 2022). Changing the pH means changing the hydrolysis and de-hydration degree, which can affect both HTC solid yield and final solid composition. In this study, the lowest Fe^{3+} concentration was chosen to be equal to a previous study (Capobianco et al., 2020), while higher values were chosen to increase the As adsorption capacity proportionally.

It should be noted that, since it is well proved that higher temperature increases carbonization (higher C content of hydrochar) (Missaoui et al., 2017), phase I of the HTC was performed at constant temperature for all treatments (200 °C), while only phase II was performed at different temperatures to assess the effect of this parameter on Fe precipitation yield and on the properties of the final hydrochar. For phase II, the temperature of 170 °C was chosen because it is the temperature tested in a previous study in a single-phase process, in which relevant problems of hydrochar instability were observed (Capobianco et al., 2020). 25 °C was set as the conventional environmental temperature, while 80 °C was chosen to have a temperature close to the water boiling point, but not equal to the boiling point, to avoid problems of excessive water evaporation. This value can be reasonably easily achieved by depressurizing the HTC reactor after phase I.

According to the factorial design, different measured outputs were collected to assess the effect of factors on the chemical and physical characteristics of the produced Fe-hydrochar. In particular, these outputs give information about the efficiency of the production process, hydrochar performances on As(V) sorption, and on the quality of the residual process water.

Considering the treatment conditions in which Fe is not added to the solution, the effect of temperature in phase II of preparation can also be assessed compared to previous results obtained in similar conditions (Di Caprio et al., 2022). In particular, no significant effect on elemental composition was evidenced in this case (Fig. S3) denoting that changing the post-treatment temperature has no significant effect ($\alpha = 0.05$) on elemental composition when Fe is not present in solution. In this case, elemental composition evidenced the following confidence intervals ($\alpha = 0.05$): 51–55% for C%, 1.3–1.1 %N, and 7.0–7.7 for H%. Considering the initial % composition of the biomass (%C = 53 ± 1%, %N = 1.6 ± 0.2%, and %H = 7.9 ± 0.2%), the determined values of %C seems to be quite low even respect to previous results in similar conditions: hydrothermal carbonization carried out at 200 °C, without acid addition, gave 58 ± 2% C in the final products (Di Caprio et al., 2022) (Fig. S3). Nevertheless, it should be considered that in this work the solid samples were also submitted to phase II in the presence of KOH to increase the pH, and the K content remaining in the solids at the end of treatment is not negligible. A correction of %C, %N, and %H was then performed removing from the final weight of products the K content and thus obtaining the output variables %C′, %N′, %H'. Even in this case, the

phase II temperature has no significant effect on %C′, %N′, and %H' (Fig. S4), meaning that the final choice on temperature treatment can be performed without considering possible effects on hydrochar composition. In this case, elemental composition evidenced the following confidence intervals (α = 0.05): 55–61% for %C′, 1.1–1.5 for %N′, and 7.6–8.5 for %H'. Considering the initial % composition of the biomass again, we noticed a significant increase in %C content after hydrothermal treatment with respect to native biomass in agreement with previous results without initial pH acidification (Di Caprio et al., 2022; Volpe and Fiori, 2017). In fact, the conditions without Fe addition correspond to an initial pH given by the deprotonation of sites onto the olive pomace, mainly carboxylic and phenolic groups (Pagnanelli et al., 2008). Pomace suspension spontaneous pH is 5.6 ± 0.2 (Di Caprio et al., 2022) and according to previous tests without acid addition, lower carbonization degrees are obtained (Pagnanelli et al., 2008).

When Fe is added to the solution, a significant effect of Fe concentration is observed on elemental composition evidencing a reduction in C, N, and H contents in the final solids as the Fe concentration in the solution increases (Fig. S5). Nevertheless, this effect could be simply due to the increase of Fe and K compounds in solids obtained for increasing Fe concentration, without any significant effect on hydrothermal reactions of carbonization determining the C, N, and H % in the final products. This was verified by calculating the corrected % elemental composition obtained by subtracting the estimated mass of Fe and K compounds in the final solids. It should be noted that the choice of reference compounds for Fe and K does not affect the statistical analysis performed, but only the analysis of the absolute values for % element. In addition, the preliminary analysis of %C contents obtained without Fe addition showed that if no correction for K is performed, %C is lower than what already obtained in similar pH conditions, then the need for such a correction was confirmed by K content and by comparison with other pomace derived HTC samples obtained in similar conditions of pH (Di Caprio et al., 2022). A similar problem was detected for HTC performed at a temperature >120 °C, due to the increased liquefaction of carbon (Kahilu et al., 2023).

Then, in the following analysis, corrected % compositions in terms of C, N and H, are determined, eliminating the contribution of Fe and K compounds to the solid mass when assessing the possible effect of factors and correlations with other measured outputs.

HTC yield in terms of the solid product obtained at the end of the two-phase preparation is an estimation of the effectiveness of hydrothermal treatment as during this phase biomass undergoes a series of reactions leading to the loss of the initial mass in the form of water (dehydration), CO_2 (decarboxylation) and soluble organic compounds (hydrolysis reactions).

Considering the addition of Fe and K, in this work, the effectiveness of HTC in terms of solid yield was estimated by subtracting the increase in mass due to the contribution of Fe and K compounds. With this approach, the corrected HTC yield (% yield') was estimated as a more appropriate output for assessing the efficiency of the hydrothermal treatment. Without this correction, yields between 65% and 90% were obtained, with higher values at higher Fe(III) concentrations (Fig. S9).

All the obtained samples have been analysed for elemental composition and the final yields of C and N in the recovered products have been calculated to estimate the carbonization efficiency in producing carbon-like materials. The efficiency target is recovering as much as possible the initial carbon of the biomass in the solid phase. According to the target of preparing a composite material containing Fe oxides, as specific sorbent compounds for As(V) removal, also the content of Fe in the solid was assessed for the different conditions. K content was also estimated because it could remain entrapped in the sorbent materials after adding KOH for Fe precipitation.

Finally, phenol concentration in the solution was considered. The process water from HTC could be used as fertilizer since it allows the recovery and extraction of mineral nutrients from the treated biomass in a sterilized solution (Celletti et al., 2021). However, some organic compounds, such as phenols, could have phytotoxic effects (Bouknana et al., 2019). Therefore, it is important to estimate the concentration of released phenols to find conditions in which phenol concentration is reduced.

The final pH was monitored for the different treatments to ensure that the amount of KOH added was sufficient to attain a pH sufficiently high to induce Fe precipitation.

The stability in water of the sorbent material was measured because it is a fundamental parameter to consider for practical applications to quantify the recovery yield and to exclude the effect of this factor on data analysis.

Fe, K, and C released in solution during the adsorption tests are other parameters measured to assess the stability in water of sorbents.

3.2. Correlation analysis

A preliminary analysis of correlation was performed to assess the effect of selected factors (temperature and Fe concentration) on all the output variables described before, and to evaluate possible correlations among these output variables.

The correlation matrix graph reporting all the linear trends and a graphical representation of the significance of correlation are reported in Fig. S6; all p-values of correlations are also reported in the matrix in Table S1.

The main emerging correlations are shown in Figs. 2 and 3, and described in the following section.

When the temperature of phase II of the process was increased, there was a reduced As(V) sorption capacity (c = −0.66, p = 0.0002). This effect could be due to more organic substances released by the solid treated at higher temperatures, which may negatively affect As(V) sorption. In particular, considering the three investigated temperature levels, a significant decrease of q is observed, only passing from 80 °C to 170 °C. In contrast, no significant difference is observed in the range 25–80 °C (Tukey HSD with 0.05 significance). This result indicates that phase II should be carried out between 25 and 80 °C without expecting a remarkable difference in q. This is a positive result for the scale-up of the process since it indicates that a specific cooling phase is not required after the reactor depressurization following phase I, thus saving energy and time. The test at 170 °C was the only one in which phase II was carried out under microwave heating. We expect that the effect of using microwave was only the heat transfer for temperature control. However, we cannot completely exclude that microwaves might have induced other unknown effects.

The increase in the temperature of phase II was correlated even with a reduction of the final pH in the residual solution (c = −0.75, p <

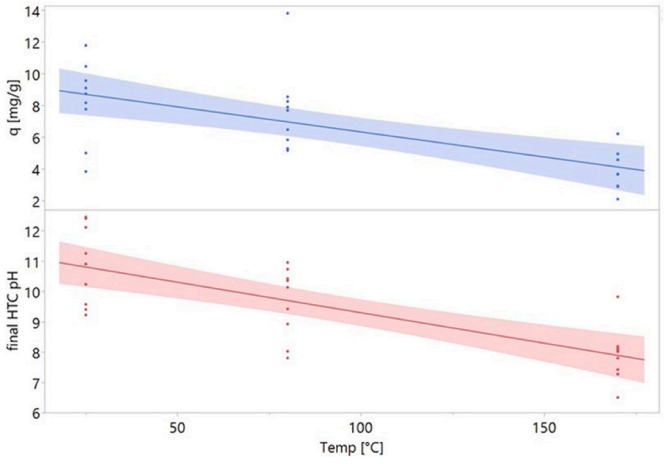

Fig. 2. Correlation between the temperature of phase II of the process and final pH and As(V) adsorption capacity (q).

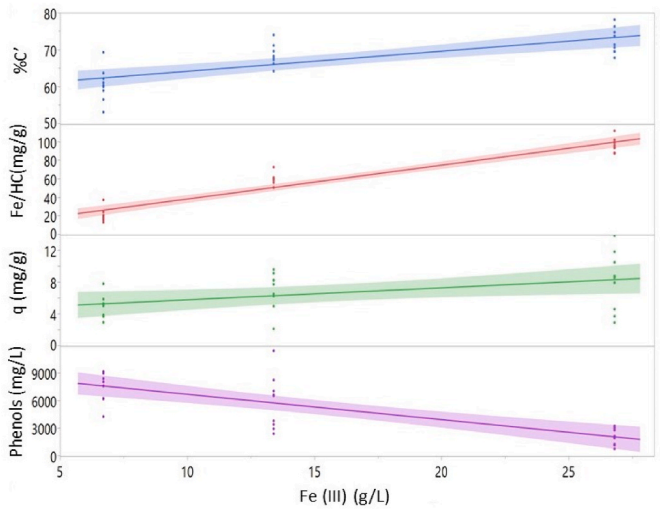

Fig. 3. A) Correlation between Fe(III) added at the beginning of the process and %C′, Fe/HC, q and phenol concentration.

0.0001). This result suggests that the increase in temperature determines the dissolution of more organic species with acid properties (Fernández-Sanromán et al., 2021). Organic acids such as acetic, formic, lactic, and others are known to be formed during HTC. They were likely responsible for this behaviour (Fernández-Sanromán et al., 2021).

The increase of the initial Fe III concentration presents a positive ($c = 0.75$) significant correlation ($p < 0.0001$) with the corrected %C (%C′) of hydrochar (Fig. 3), meaning that with increasing Fe concentration it is possible to increase the carbonization yield. This effect was in agreement with the expectations. It results from the acid property of the Fe^{3+} ion, which determines a decrease in the reaction pH during the first hydrothermal carbonization (phase I). The positive effect of low pH on carbonization yield was reported in previous studies by employing H_2SO_4 (Di Caprio et al., 2022), as H^+ concentration affects hydrolysis and de-hydration reactions necessary for carbonization. The %C′ here obtained at a higher Fe concentration is 73 ± 3%, remarkably higher than the 65% value previously obtained at a higher phase I temperature (250 °C) (Volpe and Fiori, 2017) without acid, and equal to the %C previously reported with H_2SO_4 (Di Caprio et al., 2022). This comparison shows clearly that the addition of acid can allow to use of remarkably lower temperatures in the hydrothermal phase, and that Fe^{3+} can effectively replace H_2SO_4 as a source of H^+. No significant correlation was found for initial Fe III concentration, %N′ and %H'. Higher initial Fe III concentrations even resulted in lower hydrochar yield ($c = -0.63$, $p = 0.0004$). This is a common effect when carbonization is more efficient, due to the loss of mass given by hydrolytic and de-hydration reactions. The %N yield was negatively correlated ($c = -0.72$, $p=<0.0001$) with initial Fe III concentration, likely due to the reduced pH that increases the hydrolysis of proteins. The same qualitative behaviour was found in a previous study with H_2SO_4 (Di Caprio et al., 2022).

The increment of the initial Fe III concentration induced an expected increment in the final Fe content (Fe/HC) in the solid ($c = 0.96$, $p < 0.0001$) (Fig. 3) due to the larger amount of Fe precipitates deposited during phase II. At 80 °C the increment was from 18 ± 2 mg/g for 6.7 g/L Fe(III) to 99 ± 3 mg/g when Fe(III) was increased up to 26.8 g/L. Initial Fe III concentration was positively correlated even with K content (K/HC) ($c = 0.65$; $p = 0.0002$) as KOH was added in phase II at amounts proportional to Fe(III) to convert stoichiometrically Fe^{3+} to $Fe(OH)_3$. The observed increased K content (K/HC) at higher Fe(III) concentration was probably due to a higher concentration of K^+ in the solution. Since a fraction of the solution was entrapped inside the solids, and since the hydrochar was not washed after synthesis, this inevitably resulted in increased K contents. This excessive K might be removed by adding washing procedures to the protocol. However, no washing phase was carried out in this study because no standardized protocols are available for washing hydrochar, therefore it could have been a relevant source of variability due to scarce reproducibility.

One of the most important results was the relation between Fe(III) concentration and the As(V) adsorption capacity, since an increment proportional to the Fe/HC content was expected. The increased initial Fe III concentration added in the solution increased the As(V) removal capacity (q) ($c = 0.44$, $p = 0.02$) (Fig. 3) of the obtained adsorbent, confirming the need for Fe (hydro)oxides onto carbon-like core solids to increase As(V) removal. For instance, when phase II was conducted at 25 °C, the As(V) sorption capacity increased from 2.8 ± 0.3 mg/g to 10 ± 1 mg/g when Fe III concentration supplemented increased from 0 to 26.8 g/L (Fig. S7). Interestingly, the increase in Fe concentration is negatively correlated with Fe released in water during sorption experiments ($c = -0.54$, $p = 0.0034$), meaning that the increase in Fe content (Fe/HC) is associated even with the production of a more stable material (namely, a material that releases less compounds in water). A previous study conducted without Fe precipitation, showed no correlation between q and Fe^{3+} added, in the 22–67 g/L range, likely because Fe^{3+} was not precipitated with an alkaline phase (Chen et al., 2022). However, the q values found were higher, up to 98 mg/g, due to the activation treatment performed at temperatures up to 700 °C and to the employment of a higher pH (pH 7) for arsenic adsorption tests (Chen et al., 2021a).

In this study, $FeCl_3$ was used as the source of Fe(III) because it is a widely available salt source and a cheaper source of Fe(III) with respect to other salts. Previous studies have employed even other Fe salts, such as $Fe(NO_3)_3$ (Chen et al., 2021a), but in line of principle, no relevant effect of counter ions is expected on sorption properties.

The increment of the initial Fe III concentration also determined a significant decrease of phenols in solution ($c = -0.77$, $p < 0.0001$) (Fig. 3), probably due to phenol oxidation catalysed by Fe^{3+} (Vicente et al., 2005). When the added Fe^{3+} was increased from 0 to 26.8 g/L, phenol concentration in the residual process water decreased about 6.5 folds, from about 13 g/L to 2 g/L (Fig. S8). In agreement, a negative correlation with the final pH ($c = -0.46$, $p = 0.015$) is observed (Fig. S6), meaning that the final pH decreased for increasing initial Fe III concentration in the solution. This finding can be related to phenol oxidation to carboxylic acids in solutions (Eisenhauer, 1964; Vicente et al., 2005). Typical phenolic compounds found in HTC wastewater are phenol, p-cresol, and 2,5-dimethylphenol, which were reported to be removed by the Fenton reagent (Fe^{3+} + H_2O_2) (Shen et al., 2022). Previous studies reported that in the presence of O_2, at 140–200 °C, Fe (III) and Fe(II) catalyse the oxidation of phenols in water solution. The described hypothesis about the mechanism was the production of hydroquinone and H_2O_2 from phenol oxidation by O_2, followed by the reaction of Fe(II) and Fe(III) with H_2O_2 to generate radicals (Collado et al., 2010; Vicente et al., 2005). Concerning this mechanism, it should be considered that some O_2 was available in the HTC reactor, since only 20 mL of solution were added to the 100 mL closed vessel. Further studies are required to elucidate the mechanisms involved. In addition to phenols, previous studies showed that other organic compounds typically produced and released during HTC are organic acids, furfural and hydroxymethyl furfural (Stemann et al., 2013; Weiner et al., 2014).

In addition to the correlation with the initial Fe III concentration, the corrected %C (%C′) showed negative correlations with solid yield ($c = -0.72$; $p < 0.0001$), with %N yield ($c = -0.64$, $p = 0.0003$), and Fe released ($c = -0.77$; $p < 0.0001$), and positive correlations with Fe content (Fe/HC) ($c = 0.84$, $p < 0.0001$), and K content (K/HC) ($c = 0.41$; $p = 0.0337$). In addition, %C′ is also positively correlated with %H' ($c = 0.66$; $p = 0.0002$) evidencing that in the solid there is an increase of C and H content as pH decreases, possibly due to an increased release of oxygen-containing substances and higher protonation of functional groups.

The % yield' is positively correlated with %C yield ($c = 0.64$, $p =$

0.0003) and %N yield (c = 0.72; p < 0.0001), and negatively correlated with Fe content (Fe/HC) (c = −0.73; p < 0.0001) in agreement with the already discussed negative correlation between Fe III concentration and %yield', and the positive correlation between Fe III concentration and (Fe/HC). In the same way, a negative correlation with K content (K/HC) (c = −0.50; p = 0.0079) was observed. The %yield' was also positively correlated with the release of Fe (c = 0.6; p = 0.0008). In previous studies in which different approaches to obtain Fe-hydrochar were used, the process yield was only calculated on total mass, with values between 25 and 71% (Chen et al., 2021b; Zhu et al., 2015). A large part of these values was below the yields obtained in this study (60–90%) (Fig. S9), likely because of the higher carbonization temperature employed (250–300 °C).

%N yield is positively correlated with variables that decrease for increasing Fe III concentration as phenol concentration (c = 0.55; p = 0.0028), HTC final pH (c = 0.45; p = 0.0175), and Fe release (c = 0.64; p = 0.0003), while it is negatively correlated with variables that increase for increasing Fe III concentrations, as Fe/HC (c = −0.76; p < 0.0001).

The content of Fe inside hydrochar (Fe/HC) is positively correlated with initial Fe III concentration (c = 0.96; p=<0.0001) and consequently with K content (K/HC) (c = 0.57; p = 0.0020) and As(V) sorption capacity (c = 0.42; p = 0.0304). For the same reason, Fe/HC was negatively correlated with phenols (c = −0.75; p=<0.0001), HTC pH (c = −0.51; p = 0.0061) and Fe release (c = 0.55; p = 0.0028).

The stability of hydrochar is positively correlated with the increased sorption capacity (c = 0.44; p = 0.0011) and negatively with Fe release (c = −0.60; p = 0.0011) and C release (c = −0.67; p = 0.0001) evidencing that sorption capacity increases for materials that are more stable during stirring and that instability can be due both to Fe and organics release. The stability of adsorbents has been scarcely considered in previous studies (Chen et al., 2021a, 2022; Jung et al., 2021), although it is a fundamental aspect for determining the applicability of real water treatment systems (Capobianco et al., 2020).

General findings regarding operating conditions for HTC preparation and sorption performances can be resumed in the following statements.

- Fe III concentration added at the beginning of HTC treatment should be used at the highest investigated level (26.8 g/L) because its acid property allows the preparation of hydrochar with higher %C content, with increased sorption capacity towards As(V) and increased sorbent stability in water, with reduced Fe release. In addition, increasing Fe III concentration in solution determines a remarkable reduction of the final concentration of phenols in process water, improving the quality of this effluent as a possible fertilizer. Although Fe^{3+} is a cost for the process, it should be considered that it could even be taken from sludges, since $FeCl_3$ is widely applied for sludge flocculation (Zhang et al., 2018). The hydrothermal treatment of sludge derived from flocculation with $FeCl_3$ seems very promising for the synthesis of adsorbents for As(V) removal.
- The temperature of phase II, implemented to functionalize the hydrochar with Fe, should be used in the range 25–80 °C to avoid a reduction in sorption capacity towards As(V), when higher temperatures are employed. The reason for such a reduction is not clear, but it may be due to the release of organic compounds able to bind arsenate anions in solution.

3.3. Regression analysis

A regression analysis was performed assuming a two-factor model including the interaction between Fe concentration and temperature to develop quantitative models relating the effect of factors and their interactions on relevant process outputs. This analysis was performed for all the output variables and confirmed the significance of the relations previously evidenced by correlation analysis between operating factors (Fe concentration and temperature) and outputs. A significant interaction between Fe concentration and temperature was found only for the variables 'q' and 'HTC pH', as shown in Table 1.

For some variables only the intercept (β_0) is significant (Table 1), meaning that there is not statistically significant effect induced by temperature and Fe concentration. The intercept value best estimates the output variable in the investigated temperature and Fe concentration ranges in these cases.

For As(V) sorption capacity (q), regression analysis evidenced a significant effect of Fe concentration, temperature and their interaction. This result agrees with previous correlation analyses in which the positive effect of Fe concentration and the negative effect of temperature have been evidenced. In addition, regression analysis evidenced the significant negative interaction between these two factors, meaning that the simple addition of the positive effect of Fe and the negative effect of temperature cannot explain the whole observed variability of q changing the levels of Fe and temperature. The coefficient of temperature of the empirical model to predict As(V) sorption capacity is about one order of magnitude smaller than that of Fe concentration, meaning a lower impact of temperature on q in the investigated ranges. The interaction coefficient for q is about 100 folds lower than the Fe concentration coefficient, denoting that interaction between factors was much less influencing on determining q. Nevertheless, this interaction is negative, meaning that working at higher Fe concentration and higher temperature, in addition to the decrease of q given by higher temperature, there is an additional decrease due to the interaction between temperature and Fe-concentration. The reason for this negative interaction is unknown. Still, it might be related to a positive influence of Fe on determining hydrochar hydrolysis when there are higher T and alkaline pH.

The goodness of the empirical model regressed was also assessed by lack of fit tests denoting the adequacy of the model as no significant difference can be evidenced between lack of fit variance and pure error variance. The response surface for the arsenic adsorption capacity (q) is reported in Fig. 4, allowing the identification of the combination of operating conditions (Fe concentration and temperature) necessary to obtain a Fe-hydrochar sorbent material with prescribed q value for As(V) removal. This graph and model can be used for further techno-economic assessments, to assess how the extra cost of chemical consumption (higher Fe concentration) and the reduced costs of energy consumption (lower phase II temperature) affect the final economic figures of the production process of adsorbents with different quality (q sorption). The

Table 1
Significant coefficients of regression analysis for the complete two-factor model (p < 0.0001 in all cases, except those evidenced by $^{(*)}$ where p is < 0.025). Deviations are the standard errors on regression parameters.

	β_0 (intercept)	β_1 (Temp)	β_2 ([Fe])	β_3 (Temp x [Fe])
%C'	57 ± 2	–	0.54 ± 0.09	–
%N'	1.56 ± 0.08	–	–	–
%H'	8.3 ± 0.2	–	–	–
HTC yield'	70 ± 3	–	0.6 ± 0.1$^{(*)}$	–
C yield (%)	76 ± 4	–	–	–
N yield (%)	67 ± 3	–	−0.7 ± 0.1	–
Fe/HC (mg/g)	–	–	3.6 ± 0.2	–
K/HC (mg/g)	71 ± 7	–	1.4 ± 0.3$^{(*)}$	–
Phenols (mg/L)	8350 ± 970	–	−280 ± 50	–
HTC pH	12.7 ± 0.4	−0.020 ± 0.002	−0.09 ± 0.02	0.0007 ± 0.0003$^{(*)}$
Stability (%)	68 ± 4	–	–	–
q (mg/g)	7.1 ± 0.9	−0.032 ± 0.005	0.15 ± 0.04$^{(*)}$	−0.0016 ± 0.0006$^{(*)}$
Fe release (mg/L)	4.6 ± 0.8	–	−0.13 ± 0.04$^{(*)}$	–
K release (mg/L)	140 ± 10	–	–	–
C release (mg/L)	12.3 ± 0.9	–	–	–

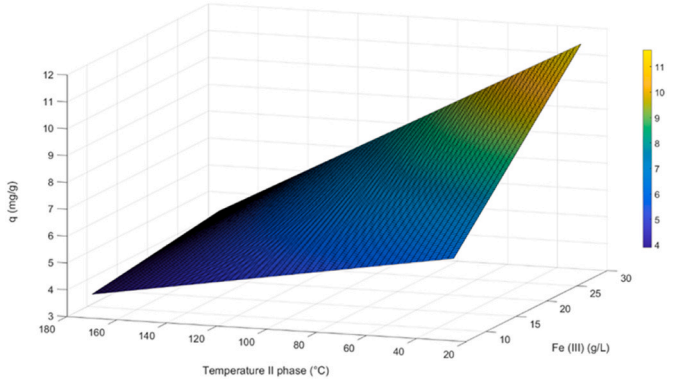

Fig. 4. Response surface plot denoting the predicted arsenic adsorption capacity (q) as a function of Fe(III) concentration and phase II temperature for the two-phase HTC process, according to what predicted by equation (7), with parameters reported in Table 1.

final market price is fundamental to allowing its application in rural areas.

Interaction is also significant for final HTC pH, but the effects are minimal, without any relevant influence on the performance of the production process.

The optimization conducted in this study allowed enhancing about three folds the arsenic adsorption capacity of the hydrochar obtained with two-phase HTC, compared to previous studies using olive pomace (Capobianco et al., 2020; Di Caprio et al., 2022). A single-phase synthesis process reported in another study reported the achievement of a higher q, till 45 mg/g, likely as a result of the utilization of different biomass (cattle manure), different pH, and of an activation carried out with thiourea (Chen et al., 2021a). The pH influences the As(V) adsorption capacity, and pH variations among different studies do not allow an easy comparison. Indeed, the study of (Chen et al., 2021a) achieved a q of 45 mg/g, at initial pH = 7, using 44.7 g/L Fe^{3+}. However, in the same study, when the adsorption test was carried out at a final pH = 5 (like in this study), the adsorbent showed a lower q of about 13 mg/g, which is comparable to the q achieved in this study with 26.8 g/L Fe^{3+} at 25–80 °C of phase II.

4. Conclusions

An innovative two-phase process for producing a low-cost adsorbent material for As(V) removal from drinking water is optimized.

The model developed allows to determine how to set phase II temperature and Fe(III) concentration to obtain a Fe-hydrochar with tailored As(V) sorption capacity and to capture the complex interplay between different variables.

The best operative conditions found are Fe concentration at the highest level (26.8 g/L) and keeping the temperature of phase II (Fe precipitation) in the range of 25–80 °C.

- Increasing the temperature of phase II up to 170 °C negatively affect the adsorption capacity of the adsorbent. We hypothesize that the alkaline hydrolysis of the hydrochar is the most likely reason. The phase II can be operated in the same reactor used for HTC at 80 °C, which would allow saving time and energy otherwise required for a complete cooling to 25 °C.
- Fe(III) at 26.8 g/L can effectively avoid the use of mineral acids or higher temperatures previously employed to achieve comparable carbonization efficiencies, thereby reducing the environmental impact of the process. Increasing Fe concentration increases the As (V) adsorption capacity (i), the stability of the adsorbent (ii), and decreases the concentration of phenolic compounds (iii). The effect (i) can be mainly imputed to the larger amount of iron hydroxides/oxides precipitated onto the hydrochar surface, while the effect (ii) can be related to the acidic property of Fe^{3+}, which determines a pH decrease and in turn a larger carbonization yield. The mechanisms responsible of the improvement of phenol removal by Fe^{3+} are likely related to a Fe^{3+} role as catalyst on oxidation reactions, however the exact mechanisms need to be better understood and elucidated in the future by specific studies.

The developed Fe-hydrochar is expected to be applicable as an alternative to conventional GFH, reducing the cost of water treatment by lowering the adsorbent cost. This innovative adsorbent is a bio-composite prepared using a largely available biomass by-product, i.e. olive pomace, as the carbon-like core for functionalizing the hydrochar with Fe, active on As(V) removal.

The results of this study can provide reference data to carry out specific techno-economic analyses to compare different process configurations.

CRediT authorship contribution statement

Fabrizio Di Caprio: Investigation, Conceptualization, Methodology, Resources, Data curation, Writing - original draft, Writing - review & editing. **Pietro Altimari:** Writing - review & editing, Supervision, Project administration. **Maria Luisa Astolfi:** Investigation, Methodology, Writing - review & editing. **Francesca Pagnanelli:** Conceptualization, Data curation, Formal analysis, Writing - original draft, Writing - review & editing, Supervision, Project administration.

Declaration of competing interest

The authors declare that they have no known competing financial interests or personal relationships that could have appeared to influence the work reported in this paper.

Data availability

Data will be made available on request.

Acknowledgement

This work was supported by the European Union in the framework of the LIFE programme (BioAs project - LIFE19 ENV/IT/000512).

Appendix A. Supplementary data

Supplementary data to this article can be found online at https://doi.org/10.1016/j.jenvman.2023.119834.

References

Agri, E., 2023. Market Situation in the Olive Oil and Table Olives Sectors Committee for the Common Organisation of the Agricultural Markets-Arable Crops and Olive Oil ([WWW Document]).

Ahsan, H., 2011. Arsenic in Drinking-Water Background Document for Development of WHO Guidelines for Drinking-Water Quality. World Health Organization.

Akar, T., Tosun, I., Kaynak, Z., Ozkara, E., Yeni, O., Sahin, E.N., Akar, S.T., 2009. An attractive agro-industrial by-product in environmental cleanup: dye biosorption potential of untreated olive pomace. J. Hazard Mater. 166, 1217–1225. https://doi.org/10.1016/J.JHAZMAT.2008.12.029.

Alshareef, S.A., Otero, M., Alanazi, H.S., Siddiqui, M.R., Khan, M.A., Alothman, Z.A., 2021. Upcycling olive oil cake through wet torrefaction to produce hydrochar for water decontamination. Chem. Eng. Res. Des. 170, 13–22. https://doi.org/10.1016/J.CHERD.2021.03.031.

Álvarez-Murillo, A., Román, S., Ledesma, B., Sabio, E., 2015. Study of variables in energy densification of olive stone by hydrothermal carbonization. J. Anal. Appl. Pyrolysis 113, 307–314. https://doi.org/10.1016/J.JAAP.2015.01.031.

Ambiente - ARPA Lazio [WWW Document], 2018. URL. https://www.arpalazio.it/. (Accessed 9 August 2023).

Azzaz, A.A., Ghimbeu, C.M., Jellai, S., El-Bassi, L., Jeguirim, M., 2022. Olive mill by-products thermochemical conversion via hydrothermal carbonization and slow pyrolysis: detailed comparison between the generated hydrochars and biochars

characteristics. Process 10 (231 10), 231. https://doi.org/10.3390/PR10020231, 2022.
Azzaz, A.A., Khiari, B., Jellali, S., Ghimbeu, C.M., Jeguirim, M., 2020. Hydrochars production, characterization and application for wastewater treatment: a review. Renew. Sustain. Energy Rev. 127, 109882 https://doi.org/10.1016/J.RSER.2020.109882.
Başakçılardan Kabakcı, S., Baran, S.S., 2019. Hydrothermal carbonization of various lignocellulosics: fuel characteristics of hydrochars and surface characteristics of activated hydrochars. Waste Manag. 100, 259–268. https://doi.org/10.1016/J.WASMAN.2019.09.021.
Benavente, V., Calabuig, E., Fullana, A., 2015. Upgrading of moist agro-industrial wastes by hydrothermal carbonization. J. Anal. Appl. Pyrolysis 113, 89–98. https://doi.org/10.1016/J.JAAP.2014.11.004.
Bouknana, D., Jodeh, S., Sbaa, M., Hammouti, B., Arabi, M., Darmous, A., Slamini, M., Haboubi, K., 2019. A phytotoxic impact of phenolic compounds in olive oil mill wastewater on fenugreek "Trigonella foenum-graecum.". Environ. Monit. Assess. 191, 1–20. https://doi.org/10.1007/S10661-019-7541-X/METRICS.
Bruxelles, 2010. IT IT COMMISSIONE EUROPEA.
Capobianco, L., Di Caprio, F., Altimari, P., Astolfi, M.L., Pagnanelli, F., 2020. Production of an iron-coated adsorbent for arsenic removal by hydrothermal carbonization of olive pomace: effect of the feedwater pH. J. Environ. Manag. 273, 111164 https://doi.org/10.1016/j.jenvman.2020.111164.
Celletti, S., Lanz, M., Bergamo, A., Benedetti, V., Basso, D., Baratieri, M., Cesco, S., Mimmo, T., 2021. Evaluating the aqueous phase from hydrothermal carbonization of cow manure digestate as possible fertilizer solution for plant growth. Front. Plant Sci. 12, 1317. https://doi.org/10.3389/FPLS.2021.687434/BIBTEX.
Chang, Q., Lin, W., Ying, W. chi, 2010. Preparation of iron-impregnated granular activated carbon for arsenic removal from drinking water. J. Hazard Mater. 184, 515–522. https://doi.org/10.1016/J.JHAZMAT.2010.08.066.
Chen, H., Xu, J., Lin, H., Wang, Z., Liu, Z., 2022. Multi-cycle aqueous arsenic removal by novel magnetic N/S-doped hydrochars activated via one-pot and two-stage schemes. Chem. Eng. J. 429, 132071 https://doi.org/10.1016/J.CEJ.2021.132071.
Chen, H., Xu, J., Lin, H., Zhao, X., Shang, J., Liu, Z., 2021a. Arsenic removal via a novel hydrochar from livestock waste co-activated with thiourea and γ-Fe2O3 nanoparticles. J. Hazard Mater. 419, 126457 https://doi.org/10.1016/J.JHAZMAT.2021.126457.
Chen, H., Xu, J., Lin, H., Zhao, X., Shang, J., Liu, Z., 2021b. Arsenic removal via a novel hydrochar from livestock waste co-activated with thiourea and γ-Fe2O3 nanoparticles. J. Hazard Mater. 126457 https://doi.org/10.1016/j.jhazmat.2021.126457.
Collado, S., Quero, D., Laca, A., Diaz, M., 2010. Fe2+-Catalyzed wet oxidation of phenolic acids under different pH values. Ind. Eng. Chem. Res. 49, 12405–12413. https://doi.org/10.1021/IE101497S.
Cope, C.O., Webster, D.S., Sabatini, D.A., 2014. Arsenate adsorption onto iron oxide amended rice husk char. Sci. Total Environ. 488, 554–561. https://doi.org/10.1016/J.SCITOTENV.2013.12.120. –489.
Di Caprio, F., Pellini, A., Zanoni, R., Astolfi, M.L., Altimari, P., Pagnanelli, F., 2022. Two-phase synthesis of Fe-loaded hydrochar for as removal: the distinct effects of initial pH, reaction time and Fe/hydrochar ratio. J. Environ. Manag. 302, 114058 https://doi.org/10.1016/J.JENVMAN.2021.114058.
Di Caprio, F., Scarponi, P., Altimari, P., Iaquaniello, G., Pagnanelli, F., 2018. The influence of phenols extracted from olive mill wastewater on the heterotrophic and mixotrophic growth of Scenedesmus sp. J. Chem. Technol. Biotechnol. 93, 3619–3626. https://doi.org/10.1002/jctb.5743.
Driehaus, W., 2002. Arsenic removal - experience with the GEH® process in Germany. Water Sci. Technol. Water Supply 2, 275–280. https://doi.org/10.2166/ws.2002.0073.
Eisenhauer, H.R., 1964. Oxidation of phenolic wastes. J. Water Pollut. Control Fed. 36, 1116–1128.
European Commission, 2019. Infringements Package: Key Decisions [WWW Document]. URL. https://ec.europa.eu/commission/presscorner/detail/EN/MEMO_19_462, 9.7.23.
Fernández-Sanromán, Á., Lama, G., Pazos, M., Rosales, E., Sanromán, M.Á., 2021. Bridging the gap to hydrochar production and its application into frameworks of bioenergy, environmental and biocatalysis areas. Bioresour. Technol. 320, 124399 https://doi.org/10.1016/J.BIORTECH.2020.124399.
Gimenez, M., Rodríguez, M., Montoro, L., Sardella, F., Rodríguez-Gutierrez, G., Monetta, P., Deiana, C., 2020. Two phase olive mill waste valorization. Hydrochar production and phenols extraction by hydrothermal carbonization. Biomass Bioenergy 143, 105875. https://doi.org/10.1016/J.BIOMBIOE.2020.105875.
He, R., Peng, Z., Lyu, H., Huang, H., Nan, Q., Tang, J., 2018. Synthesis and characterization of an iron-impregnated biochar for aqueous arsenic removal. Sci. Total Environ. https://doi.org/10.1016/j.scitotenv.2017.09.016.
Jadhav, S.V., Bringas, E., Yadav, G.D., Rathod, V.K., Ortiz, I., Marathe, K.V., 2015. Arsenic and fluoride contaminated groundwaters: a review of current technologies for contaminants removal. J. Environ. Manag. 162, 306–325. https://doi.org/10.1016/J.JENVMAN.2015.07.020.
Jovanovic, D., Jakovljević, B., Rašić-Milutinović, Z., Paunović, K., Peković, G., Knezević, T., 2011. Arsenic occurrence in drinking water supply systems in ten municipalities in Vojvodina Region, Serbia. Environ. Res. 111, 315–318. https://doi.org/10.1016/J.ENVRES.2010.11.014.
Jung, K.W., Lee, S.Y., Choi, J.W., Hwang, M.J., Shim, W.G., 2021. Synthesis of Mg–Al layered double hydroxides-functionalized hydrochar composite via an in situ one-pot hydrothermal method for arsenate and phosphate removal: structural characterization and adsorption performance. Chem. Eng. J. 420, 129775 https://doi.org/10.1016/J.CEJ.2021.129775.
Kahilu, G.M., Bada, S., Mulopo, J., 2023. Systematic physicochemical characterization, carbon balance and cost of production analyses of activated carbons derived from (Co)-HTC of coal discards and sewage sludge for hydrogen storage applications. Waste Dispos. Sustain. Energy 52 (5), 125–149. https://doi.org/10.1007/S42768-023-00136-4, 2023.
Katsoyiannis, I.A., Mitrakas, M., Zouboulis, A.I., 2015. Arsenic occurrence in Europe: emphasis in Greece and description of the applied full-scale treatment plants. Desalin. Water Treat. 54, 2100–2107. https://doi.org/10.1080/19443994.2014.933630.
Libra, J.A., Ro, K.S., Kammann, C., Funke, A., Berge, N.D., Neubauer, Y., Titirici, M.M., Fühner, C., Bens, O., Kern, J., Emmerich, K.H., 2011. Hydrothermal carbonization of biomass residuals: a comparative review of the chemistry, processes and applications of wet and dry pyrolysis. Biofuels. https://doi.org/10.4155/bfs.10.81.
Luong, V.T., Cañas Kurz, E.E., Hellriegel, U., Luu, T.L., Hoinkis, J., Bundschuh, J., 2018. Iron-based subsurface arsenic removal technologies by aeration: a review of the current state and future prospects. Water Res. 133, 110–122. https://doi.org/10.1016/J.WATRES.2018.01.007.
Martín-Lara, M.A., Pagnanelli, F., Mainelli, S., Calero, M., Toro, L., 2008. Chemical treatment of olive pomace: effect on acid-basic properties and metal biosorption capacity. J. Hazard Mater. 156, 448–457. https://doi.org/10.1016/J.JHAZMAT.2007.12.035.
Medunić, G., Fiket, Ž., Ivanić, M., 2020. Arsenic contamination status in europe, Australia, and other parts of the World. In: Srivastava, S. (Ed.), Arsenic in Drinking Water and Food. Springer, Singapore, pp. 188–233. https://doi.org/10.1007/978-981-13-8587-2_6.
Missaoui, A., Bostyn, S., Belandria, V., Cagnon, B., Sarh, B., Gökalp, I., 2017. Hydrothermal carbonization of dried olive pomace: energy potential and process performances. J. Anal. Appl. Pyrolysis 128, 281–290. https://doi.org/10.1016/J.JAAP.2017.09.022.
Mourão, P.A.M., Di Caprio, F., Cansado, I.P.P., Castanheiro, J.E., Falcone, I., Astolfi, M. L., Altimari, P., Pagnanelli, F., 2022. Granulation and activation of an arsenic adsorbent made of iron oxide doped hydrochar. Chem. Eng. Trans. 93, 91–96. https://doi.org/10.3303/CET2293016.
Nuhoglu, Y., Malkoc, E., 2009. Thermodynamic and kinetic studies for environmentaly friendly Ni(II) biosorption using waste pomace of olive oil factory. Bioresour. Technol. 100, 2375–2380. https://doi.org/10.1016/J.BIORTECH.2008.11.016.
Pagnanelli, F., Mainelli, S., Toro, L., 2008. New biosorbent materials for heavy metal removal: product development guided by active site characterization. Water Res. 42, 2953–2962. https://doi.org/10.1016/J.WATRES.2008.03.012.
Pagnanelli, F., Mainelli, S., Vegliò, F., Toro, L., 2003. Heavy metal removal by olive pomace: biosorbent characterisation and equilibrium modelling. Chem. Eng. Sci. 58, 4709–4717. https://doi.org/10.1016/J.CES.2003.08.001.
Sappa, G., Ergul, S., Ferranti, F., 2014. Geochemical modeling and multivariate statistical evaluation of trace elements in arsenic contaminated groundwater systems of Viterbo Area, (Central Italy). SpringerPlus 3, 1–19. https://doi.org/10.1186/2193-1801-3-237/TABLES/8.
Shen, T., Yan, M., Xia, Y., Hu, R., Yang, Y., Chen, C., Chen, F., Hantoko, D., 2022. Treatment of wastewater from food waste hydrothermal carbonization via Fenton oxidization combined activated carbon adsorption. Waste Dispos. Sustain. Energy 4, 205–218. https://doi.org/10.1007/S42768-022-00106-2/METRICS.
Sorg, T.J., Chen, A.S.C., Wang, L., 2014. Arsenic species in drinking water wells in the USA with high arsenic concentrations. Water Res. 48, 156–169. https://doi.org/10.1016/J.WATRES.2013.09.016.
Stemann, J., Putschew, A., Ziegler, F., 2013. Hydrothermal carbonization: process water characterization and effects of water recirculation. Bioresour. Technol. 143, 139–146. https://doi.org/10.1016/J.BIORTECH.2013.05.098.
Tarhan, S.Z., Koçer, A.T., Özçimen, D., Gökalp, İ., 2021. Cultivation of green microalgae by recovering aqueous nutrients in hydrothermal carbonization process water of biomass wastes. J. Water Process Eng. 40 https://doi.org/10.1016/J.JWPE.2020.101783.
Ungureanu, G., Santos, S., Boaventura, R., Botelho, C., 2015. Arsenic and antimony in water and wastewater: overview of removal techniques with special reference to latest advances in adsorption. J. Environ. Manag. 151, 326–342. https://doi.org/10.1016/j.jenvman.2014.12.051.
Vicente, J., Rosal, R., Díaz, M., 2005. Catalytic wet oxidation of phenol with homogeneous iron salts. J. Chem. Technol. Biotechnol. 80, 1031–1035. https://doi.org/10.1002/JCTB.1280.
Volpe, M., Fiori, L., 2017. From olive waste to solid biofuel through hydrothermal carbonisation: the role of temperature and solid load on secondary char formation and hydrochar energy properties. J. Anal. Appl. Pyrolysis 124, 63–72. https://doi.org/10.1016/j.jaap.2017.02.022.
Wang, L., Chi, Y., Du, K., Zhou, Z., Wang, F., Huang, Q., 2023. Hydrothermal treatment of food waste for bio-fertilizer production: regulation of humus substances and nutrient (N and P) in hydrochar by feedwater pH. Waste and Biomass Valorization 1, 1–15. https://doi.org/10.1007/S12649-023-02033-7/TABLES/4.
Wang, S., Gao, B., Zimmerman, A.R., Li, Y., Ma, L., Harris, W.G., Migliaccio, K.W., 2015. Removal of arsenic by magnetic biochar prepared from pinewood and natural hematite. Bioresour. Technol. 175, 391–395. https://doi.org/10.1016/j.biortech.2014.10.104.
Wang, S., Mulligan, C.N., 2006. Natural attenuation processes for remediation of arsenic contaminated soils and groundwater. J. Hazard Mater. 138, 459–470. https://doi.org/10.1016/J.JHAZMAT.2006.09.048.
Wei, Y., Wei, S., Liu, C., Chen, T., Tang, Y., Ma, J., Yin, K., Luo, S., 2019. Efficient removal of arsenic from groundwater using iron oxide nanoneedle array-decorated biochar fibers with high Fe utilization and fast adsorption kinetics. Water Res. 167, 115107 https://doi.org/10.1016/J.WATRES.2019.115107.

Weiner, B., Poerschmann, J., Wedwitschka, H., Koehler, R., Kopinke, F.-D., 2014. Influence of Process Water Reuse on the Hydrothermal Carbonization of Paper. https://doi.org/10.1021/sc500348v.

WHO TEAM Water, Sanitation, H., 2018. Arsenic Primer, Arsenic Primer Guidance on the Investigation and Mitigation of Arsenic Contamination.

Xu, Z., Sun, M., Xu, X., Cao, X., Ippolito, J.A., Mohanty, S.K., Ni, B.J., Xu, S., Tsang, D.C. W., 2023. Electron donation of Fe-Mn biochar for chromium(VI) immobilization: key roles of embedded zero-valent iron clusters within iron-manganese oxide. J. Hazard Mater. 456, 131632 https://doi.org/10.1016/J.JHAZMAT.2023.131632.

Xu, Z., Wan, Z., Sun, Y., Cao, X., Hou, D., Alessi, D.S., Ok, Y.S., Tsang, D.C.W., 2021. Unraveling iron speciation on Fe-biochar with distinct arsenic removal mechanisms and depth distributions of as and Fe. Chem. Eng. J. 425, 131489 https://doi.org/10.1016/J.CEJ.2021.131489.

Xu, Z., Wan, Z., Sun, Y., Gao, B., Hou, D., Cao, X., Komárek, M., Ok, Y.S., Tsang, D.C.W., 2022. Electroactive Fe-biochar for redox-related remediation of arsenic and chromium: distinct redox nature with varying iron/carbon speciation. J. Hazard Mater. 430, 128479 https://doi.org/10.1016/J.JHAZMAT.2022.128479.

Zhang, H., Xue, G., Chen, H., Li, X., 2018. Magnetic biochar catalyst derived from biological sludge and ferric sludge using hydrothermal carbonization: preparation, characterization and its circulation in Fenton process for dyeing wastewater treatment. Chemosphere 191, 64–71. https://doi.org/10.1016/J.CHEMOSPHERE.2017.10.026.

Zhang, X., Zhao, K., Shi, X., Tian, Z., Huang, Z., Zhao, L., 2022. Novel strategy for reusing agricultural mulch film residual by iron modification for arsenic removal in gold-smelting wastewater. Front. Chem. 10, 1348. https://doi.org/10.3389/FCHEM.2022.1036726/BIBTEX.

Zhu, X., Qian, F., Liu, Y., Zhang, S., Chen, J., 2015. Environmental performances of hydrochar-derived magnetic carbon composite affected by its carbonaceous precursor. RSC Adv. 5, 60713–60722. https://doi.org/10.1039/C5RA07339A.

Zubair, Y.O., Fuchida, S., Tokoro, C., 2020. Insight into the mechanism of arsenic(III/V) uptake on mesoporous zerovalent iron-magnetite nanocomposites: adsorption and microscopic studies. ACS Appl. Mater. Interfaces 12, 49755–49767. https://doi.org/10.1021/ACSAMI.0C14088/ASSET/IMAGES/LARGE/AM0C14088_0013.JPEG.